

# Strömgren $uvby - \beta$ photometry towards the region of the Cometary Globules CG 30/31/38\*

A.S. Nielsen, H. Jönch-Sørensen, and J. Knude

Niels Bohr Institute for Astronomy, Geophysics and Physics, Juliane Maries Vej 32, 2100 København Ø, Denmark (alan@astro.ku.dk)

Received 24 March 2000 / Accepted 26 April 2000

**Abstract.** With the Danish 1.54 m telescope at La Silla, Chile, we have obtained deep ( $V \approx 19^m$ ) CCD frames in the  $uvby - \beta$  Strömgren system towards the region of the cometary globules CG 30/31/38. Also, a nearby reference field, with a minor amount of visible molecular material, has been observed in order to estimate the expected *normal* foreground reddening in this direction of the Galaxy. We have obtained complete  $uvby - \beta$  information for 698 and 526 stars in these two regions, respectively, allowing a determination of individual stellar extinctions and distances for the A- to G-type star subsample meeting the criteria in the calibrations. A lower envelope in the distance–reddening diagram ( $r - E(b - y)$ ) indicates that the minimum total absorption through half the Galactic disk along the line of sight is  $A_V \approx 1^m3$  in this direction. The distance to the CG 30/31/38 complex is not directly derived from the  $r - E(b - y)$ -diagram but two faint foreground M-dwarfs are identified, and based on the obtained  $V$ , ( $V - I$ ) photometry a lower distance limit of  $215 \pm 40$  pc is derived.

We also report the discovery of a galaxy seen in  $V$  and  $I$ -band exposures in spite of the high extinction, located at the very low galactic latitude of  $b \sim -1.6^\circ$ .

**Key words:** ISM: clouds – ISM: dust, extinction

## 1. Introduction

Cometary globules are small molecular clouds, consisting mostly of  $H_2$ , and have a striking resemblance to solar system comets due to ionization and strong stellar winds from nearby massive stars. Hawarden & Brand (1976) first described and defined them as a sub-group of Bok globules. The observed globule masses are in the range from 1–100  $M_\odot$  and the size of the shock-compressed bright-rimmed head is typically between 0.1–1.0 pc. The tail consists of photo evaporated material from the globule by the incident ionizing radiation and points directly away from the massive stars. Optically they appear as dark patches against the stellar background, and always with extremely high visual extinction. Very intense investigations through more than 15 years in the optical, infrared and at radio

wavelengths have given evidence that low mass star formation is indeed taking place in the densest parts of the globules, that are shielded from the general interstellar radiation field (Bhatt 1993). The formation and evolution of cometary globules due to radiation driven implosions (RDI) was treated analytically by Bertoldi (1989) and Bertoldi & McKee (1990). The RDI model is based on the *rocket effect* introduced by Oort & Spitzer (1955), whereby the ionized gas expands into the interstellar medium and an ionization front preceded by a shock in the neutral gas propagates into the cloud. This shock may well trigger the formation of a star in the head of the cometary globule. That scenario has been supported by Lefloch & Lazareff (1994, 1995) and more recently by Lefloch et al. (1997), discussing the RDI model in much more detail than previously, using both numerical hydrodynamics and simple analytical modeling.

A major fraction of CG's are located in the direction of the Gum Nebula, a large region of ionized gas, seen in deep  $H\alpha$  and [NII] emission exposures, on the southern sky centred at  $(l, b) \sim (258^\circ, -2^\circ)$ . In the spectacular complex of cometary globules, CG 30/31/38, only CG 30 hosts an infrared source (CG 30-IRS4) and the Herbig-Haro object HH 120 (Pettersson 1984). The position of CG 30 is  $(\alpha, \delta)_{2000} = (08^h 09^m 32^s.8, -36^\circ 05' 13'')$  and  $(l, b) = (253.3^\circ, -1.6^\circ)$ . Nielsen et al. (1998) estimated the total mass of the CG complex, based on  $^{13}CO$  measurements, to be  $\approx 43 M_\odot$  and discovered a dense molecular outflow with a modest mass of 0.3  $M_\odot$  associated with CG 30, which is also an indication of recent star formation inside the cloud. The physical parameters were derived assuming a distance of 450 pc to the CG's, which traditionally has been used in the literature. For a long time it has been assumed that the cometary globules were somehow associated with the Gum Nebula, but this could be a coincidence due to projection effects. Sahu (1992) suggests a physical relationship between the CG's and the IRAS Vela Shell - an infrared emitting dusty shell, centred at  $l \approx 263^\circ, b \approx -7^\circ$ , suggested to be at a distance of 450 pc. Furthermore she proposed a distance of 800 pc to the center of the nebula. The IRAS Vela Shell, having an average radius of  $\approx 7.5^\circ$ , envelope the old Vela OB2 association on the verge of disintegration (age  $\sim 30$  Myr; Sahu 1992), and is probably a remnant GMC. The appearance of the CG's in that region is presently maintained by radiation pressure from massive stars like  $\zeta$ -Puppis (O4f), the  $\gamma^2$ -Velorum system (WC8 +

\* Based on observations ESO, La Silla

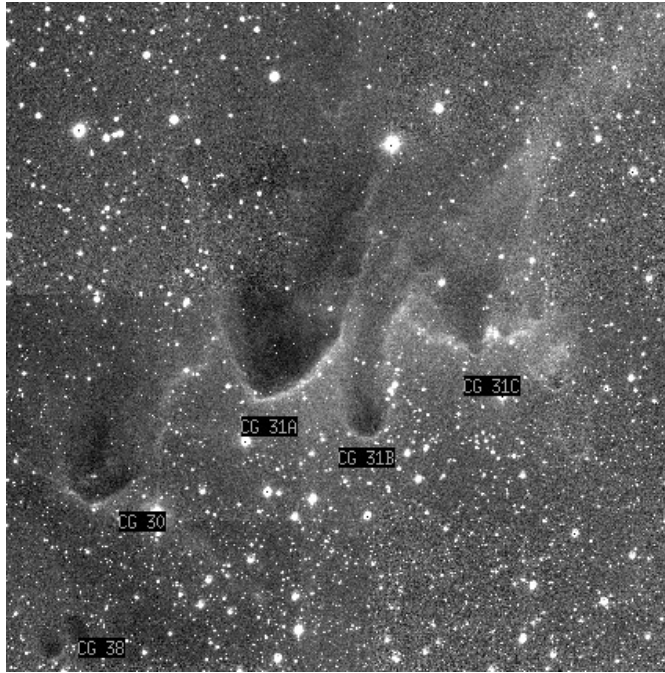


**Fig. 1.** A mosaic of 5  $\beta_{\text{narrows}}$  frames showing the region of the cometary globules CG 30/31/38 that we have observed. The size of the field ( $23' \times 23'$ ) corresponds to 4 CCD frames arranged in a square around the position of CG 31A. The fifth frame is overlapping the other four frames.

O8III) and the nearby Vela OB2 association believed to be approximately at the centre of the Gum Nebula seen in projection. Due to the connection of these sources to the CG's, Brandt et al. (1971) estimated a distance to the globules of 400–450 pc. Recently, de Zeeuw et al. (1999) have estimated the distance to the centre of Vela OB2 to be  $410 \pm 12$  pc on the basis of proper motion and Hipparcos parallaxes, in agreement with previous results. Franco (1990) discovered a feature in the  $r - E(b - y)$ -diagram, having a distance of  $200 \pm 20$  pc, which he proposed to be the near edge of the Gum Nebula resulting in a distance of  $290 \pm 30$  pc to its centre assuming an angular radius of  $90 \pm 10$  pc. This result is in agreement with Gott & Ostriker (1971) estimating the distance to the near edge of the nebula of 230 pc (330 pc to the center, assuming  $18^\circ$  as its angular radius).

The distance to  $\zeta$ -Pup and  $\gamma^2$ -Vel has been re-assessed by van der Hucht (1997) to be  $429^{+120}_{-77}$  pc ( $\pi = 2.33 \pm 0.51$  mas) and  $258^{+41}_{-31}$  pc ( $\pi = 3.88 \pm 0.53$  mas), respectively, based on direct Hipparcos parallax measurements. This will put  $\zeta$ -Pup to the back of the Gum Nebula, whereas  $\gamma^2$ -Vel is close to the centre. However, the small number of objects observed believed conclusively to be part of Vela OB2 combined with the large distance spread of member stars (200–650 pc) determined from parallaxes, this association seems to be quite loosely defined. What is still missing is a clear relationship between distance, origin and the spatial distribution of important objects in this region (the Gum Nebula, Vela OB2, Vela R2 (a young association at a distance of  $\sim 800$  pc),  $\zeta$ -Pup,  $\gamma^2$ -Vel and the SNR's) and their possible relation, is still a matter of debate and rather con-

troversial (Schaerer et al. 1997). Establishing direct distances to molecular clouds, in order to determine accurate physical parameters obtained from radio/IR measurements, is generally rather complicated, but of great importance. Knude et al. (1999) have estimated the distance to the CG 30/31/38 complex based on shifting a new  $(V - I)_0 - M_V$  relation using Hipparcos data to fit confining trends in the  $(V - I) - V$ -diagram. This is the first attempt ever to derive a direct distance to the globules, and the authors find a feature at a distance of  $\sim 200$  pc with a visual extinction  $A_V \sim 3^m6$ , identified as the tail of CG 31. That will put the CG 30/31/38 complex at a distance of  $\sim 200$  pc from us, and also from the Vela OB2. Possibly, this result will have important implications for the previous published radio/IR data presented by several authors (Nielsen et al. (1998) and references therein).

The very well calibrated Strömrgren  $uvby - \beta$  intermediate - narrow - band photometric system, is especially suitable for deriving physical parameters like  $T_{\text{eff}}$ ,  $[\text{Fe}/\text{H}]$ ,  $M_V$ ,  $\log(g)$  and intrinsic colours mainly for F and early G-type stars (Strömrgren 1963). The  $\beta$  index is defined as the difference between the two bands  $\beta_{\text{narrows}} - \beta_{\text{wide}}$  centered at the same effective wavelength on the  $H\beta$  line.  $\beta$  is thus not affected by interstellar reddening and measures  $T_{\text{eff}}$  for stars ranging from early A- to mid G-type.

From Strömrgren photometry it is possible to derive several physical parameters like distance and reddening for individual stars. For a field size of  $0.25^\circ$  one would expect to have  $\approx 10$  A3–G2 stars within 450 pc, some of which might have a favourable location with respect to the globules' tails. In principle this will allow an estimate of the distance to e.g. dust features like cometary globules; a most important, but a rarely available parameter, when determining physical properties of molecular clouds from e.g. radio data. Such distances are most often determined by the clouds' association with something with a known distance (Henning & Launhardt 1998).

## 2. Observations and data reductions

The data were obtained during an observing run at La Silla, Chile, during Feb/Mar 1997 using DFOSC at the danish 1.54 m telescope. At the time of observations the DFOSC was equipped with a thinned Loral  $2k \times 2k$  W11/4 CCD. Each CCD frame covers an area of  $13' \times 13'$ .

However, since the Strömrgren filters were only 60 mm in diameter vignetting of the field is imposed (see Fig. 6) when filters are mounted in the FASU (filter and shutter unit). This was necessary because the internal filters in the DFOSC are tilted in order to avoid reflections. For interference filters the result is a shift in effective wavelength across the field of view which is serious for intermediate- to narrow band filters as the ones used here. The effective clear aperture of the  $uvby - \beta$  filters were accordingly limited to approximately 60% of the full CCD frame.

The areas observed were the CG 30/31/38 complex (see Fig. 1) and a nearby reference field without any obvious absorption features of approximately half the field size, corresponding

**Table 1.** Exposure times in minutes

$u$	$v$	$b$	$y$	$\beta_n$	$\beta_w$
$2 \times 45$	30	10	15	45	15

to 2 DFOSC fields. In both fields we obtained deep photometry in  $uvby$ ,  $\beta_{narrow}$ , and  $\beta_{wide}$  bands. In addition to the longest exposures a sequence of frames with shorter exposure times were obtained in order to tie-in both the bright and faint stars in the field. Typically, we needed 3–4 exposures in each field in each band, fewest in  $u$  where we very seldom experience problems with saturated stars. The longest exposure times were slightly adjusted according to the atmospheric conditions on the actual night, and in Table 1 we list the typical longest exposure times. In addition, we also performed extensive  $V$  and  $I$  observations of the same region, and the results have been discussed in Knude et al. (1999). Furthermore, we have recently obtained a few deep  $V$  and  $I$  exposures, in order to identify very faint stars in front of the dense head of the globules, allowing us to estimate a lower distance limit (see Sect. 6.3).

The CG 30/31/38 field was centered on the position  $(08^h08^m53^s0, -36^\circ00'00'')_{2000}$  and  $(l, b) = (253.2^\circ, -1.7^\circ)$  with four overlapping CCD frames arranged in a square around this position and a central field on the center position, thus overlapping all of the other four fields. As a consequence, stars of intermediate magnitude may have been observed in 4 frames in each colour and four neighbouring fields yielding a total of 8 observations, but the typical number of observations for stars with  $V \approx 13^m - 19^m$  is 3.

The reference field was situated at the same galactic latitude as the CG 30/31/38 field at  $l = 251.2^\circ$ . Three overlapping CCD fields were observed, shifted  $6'$  in  $\alpha$ . Thus, the number of observations are generally lower for stars in the reference field compared to the CG 30/31/38 field. In this field we covered an area on the sky of  $625 \square'$  and for the reference field the observed area was  $330 \square'$ .

All reductions have been performed using the standard Image Reduction and Analysis Facility (IRAF) packages. The raw frames were treated in the common manner: after removing bad pixels and columns, we subtracted the bias and divided the frames by a normalized sky flat field. The contribution from dark current ( $\sim 4e^-/30$  min) could be neglected since no structure was present after bias subtraction. The sources were identified and counted using the DAOFIND routine and the resulting coordinate files were edited to remove non-stellar objects and artifacts misidentified as stars and to append stellar sources that were not originally extracted by the finding routine. The actual photometry was performed by using the DAOPHOT package including both aperture and point spread function fitting photometry.

When analysing the final photometry files we noticed some problems with the  $c_1$ -index at the western part of the reference field. We traced this problem to be associated with the flat fielding in the  $u$  band, and in the following analysis we restrict the data to the eastern  $\approx 60\%$  of the reference field where the  $c_1$ -

index is reliable and we may derive physical parameters like  $E(b-y)$ ,  $M_V$  etc. Thus, the area on the sky from where we have  $E(b-y)$  and distance information in the reference field is only  $\approx 1/3$  of the CG 30/31/38 field. However, the problem is limited to the  $u$  frame, so when we discuss other bands e.g. the  $(b-y) - V$ -diagrams we may use the full reference field.

### 2.1. Photometry

In each programme field CG 30/31/38 and the reference field, overlapping frames were obtained and common instrumental systems were established by determining frame offsets in each band from the stars in common. Thus, any frame then defines its own *system* which is connected to neighbouring fields by adding offsets determined from stars in overlapping areas. Extinction corrections do not enter the process of establishing an instrumental system because all frames in the individual magnitudes in a given direction are connected onto a common instrumental system using overlapping frames.

One full night of photometric quality was devoted to observe standard stars and selected frames in the programme fields and thus connecting the instrumental systems to the standard system. On two more nights some additional time was used to observe standard stars in order to check the quality of the transformations. Extinction coefficients were supplied by the danish 0.5 m telescope (Strömgren Automatic Telescope abbreviated SAT).

### 2.2. Standard stars

In the  $uvby - \beta$  system most primary standard stars (Crawford & Barnes 1970, Grønbech et al. 1976, Olsen 1983, and Perry et al. 1987) are normally too bright to be observed with a telescope like the danish 1.54 m, since the CCD will saturate in a few seconds, thus one may have to rely on fainter, secondary standard stars. However, using the defocusing necessary, a few primary standard stars were selected for observations in order to check the reliability of the transformations derived from the secondary standards. Our sources of secondary standards (20) were taken from Jönch-Sørensen (1993) and Schuster & Nissen (1988). These two set are closely transformed to the primary standard system, and beside being fainter, and thus more easily observable, they represent an extension to both more evolved and more metal poor stars compared to the primary standard stars. The selected standard stars were in the range  $0^m02 \leq (b-y) \leq 0^m70$  and  $2^m55 \leq \beta \leq 2^m92$  matching the A- to early G-type stars (LC III–V) that we planned to use for deriving accurate distances and reddening. The standard stars were of  $V$  magnitudes between  $6^m5$  and  $10^m9$  with metallicities ( $[Fe/H]$ ) between approximately  $-1.0$  and  $0.3$  dex. As stressed by e.g. Crawford and Barnes (1970) and Manfroid & Sterken (1992) it is important to observe standard stars of nearly the same spectral types, colours and luminosities as the programme stars.

From the photometry we derived the following parameters in the instrumental system: the colour index  $(b-y)$ ,  $V$  the visual magnitude,  $m_1 = (v-b) - (b-y)$ , a measure of the strength of metal lines, and  $c_1 = (u-v) - (v-b)$  which is a measure of the

strength of the Balmer discontinuity, and the  $\beta$ -index measuring the strength of the H $\beta$  line in a star's spectrum. After correcting for extinction we derived the following transformations in the standard system following the procedure outlined by Crawford (1975):

$$\begin{aligned}(b - y)_{\text{std}} &= 1.022(b - y)_{\text{inst}} + 0.784[0^{\text{m}}007] \\ V_{\text{std}} &= 1.004y_{\text{inst}} - 3.798[0^{\text{m}}013] \\ (m_1)_{\text{std}} &= 1.111(m_1)_{\text{inst}} - 0.128(b - y)_{\text{std}} \\ &\quad - 1.276[0^{\text{m}}008] \\ (c_1)_{\text{std}} &= 1.070(c_1)_{\text{inst}} + 0.362(b - y)_{\text{std}} \\ &\quad - 0.887[0^{\text{m}}012] \\ \beta_{\text{std}} &= 1.586\beta_{\text{inst}} + 0.377[0^{\text{m}}010]\end{aligned}$$

The numbers in brackets indicate the  $\sigma$  of the fit in the transformations. The only noticeable difference from our previous experience with standard transformation of CCD  $uvby - \beta$  photometry is the absence of any significant colour term in the  $V$ -transformation. In the previous reductions (see e.g. Jønch-Sørensen 1994 and Jønch-Sørensen & Knude 1994) we have found colour terms of the order 0.01 to 0.02, but in the present work the colour term was absent.

Using the frames in the programme fields that were observed during the same night as the standard stars, new zero points were derived for each instrumental system (corresponding to each programme field) using the above mentioned slopes and colour terms. In the CG 30/31/38 field 27 stars were used to derive the zero point and thus the final transformation. The standard error of the mean ( $\sigma/\sqrt{N}$ ) of the zero points were  $0^{\text{m}}004$ ,  $0^{\text{m}}003$ ,  $0^{\text{m}}009$ ,  $0^{\text{m}}018$  and  $0^{\text{m}}010$  for  $(b - y)$ ,  $V$ ,  $m_1$ ,  $c_1$  and  $\beta$ , respectively.

The  $V$  and  $I$  data have been discussed in Knude et al. (1999) and the transformations derived there were as follows (data from 1997):

$$V_{\text{std}} = V_{\text{inst}} + 0.022(V - I)_{\text{std}} - 1.378 [0.033]$$

$$(V - I)_{\text{std}} = 0.973(V - I)_{\text{inst}} + 0.932 [0.030]$$

based on 29 standard stars (Graham 1982, Landolt 1983).

For the new data obtained in Nov. 1999, we derived transformations from the instrumental system to the standard system using 15 stars already transformed in previous data for  $V_{\text{std}}$  and  $(V - I)_{\text{std}}$ :

$$V_{\text{std}} = V_{\text{inst}} + 0.036(V - I)_{\text{std}} - 1.067 [0.050]$$

$$(V - I)_{\text{std}} = 1.018(V - I)_{\text{inst}} + 1.006 [0.050]$$

For 2953 stars in the CG 30/31/38 field, we compared  $V$  magnitudes from  $uvby$ - and  $V, I$  photometry, and found that they agreed within  $0^{\text{m}}06$  in rms with no residual trends as a function of colour,  $(b - y)$  or  $(V - I)$ , removing our concern regarding the absent colour term in the  $y$  to  $V$  transformation mentioned above.

### 3. Calibration of $(b - y)_0$ and $M_V$

Intrinsic colour and  $M_V$  can be estimated in the  $uvby - \beta$  system for stars of spectral types ranging from B to early/mid G-type stars, excluding A1 and A2 stars (Crawford 1975, Crawford 1979, Olsen 1988, and Schuster & Nissen 1989).

Stars were roughly classified into B, A, F and G type stars using  $(b - y)$ ,  $\beta$ ,  $[m_1]$  and  $[c_1]$ , where  $[m_1] = m_1 + 0.3(b - y)$  and  $[c_1] = c_1 - 0.2(b - y)$  are two indices not affected by reddening if the reddening law is normal, which we suppose it is. The procedure we used was as follows:

B-stars were defined as stars having  $[m_1] < 0^{\text{m}}15$  or  $(b - y) < 0^{\text{m}}$ . A-stars have  $2^{\text{m}}72 \leq \beta \leq 2^{\text{m}}89$  and  $[m_1] > 0^{\text{m}}15$ . Stars around the Balmer maximum (type A1-A2 are not used in this work), often referred to as the *intermediate group*, are defined as stars having  $[m_1] < 0^{\text{m}}221$ ,  $[c_1] > 0^{\text{m}}917$  and not being A- or B-stars. The F-star group is defined as stars not being any of the former types and having  $2^{\text{m}}58 \leq \beta \leq 2^{\text{m}}72$ . Note that what we call F-stars thus includes early G-type stars, approximately to G2. Finally, stars with  $2^{\text{m}}55 \leq \beta < 2^{\text{m}}58$  are classified as G-stars. After this classification  $(b - y)_0$  and  $M_V$  were derived for the A-stars using the calibration by Crawford (1979). For the F-stars  $(b - y)_0$  are calculated from the calibration by Olsen (1988) and  $M_V$  from Crawford (1975). Note that we have extended the validity of the calibration by Crawford (1975) slightly from  $\beta = 2.59$  to  $\beta = 2.58$ . The calibration by Schuster and Nissen (1989) was used to derive  $(b - y)_0$  for the G-type stars. This calibration is also valid for F-stars, but in order to keep consistency with previous results we prefer the Crawford (1975) calibration for those stars. A comparison of the two calibrations applicable to F-stars derived by Olsen (1988) and Schuster & Nissen (1989) can be found in Jønch-Sørensen (1994). Absolute visual magnitudes for the G-type stars were found using the calibration by Olsen (1984). The decrease of temperature dependence of the  $\beta$ -index for these cool stars means that  $(b - y)_0$  has to be used instead of  $\beta$  as a temperature indicator. Olsen (1984) states this as a preliminary calibration, but we still consider it as the best choice, because of the tight connection to the Crawford (1975) calibration and the standard dwarf sequence for F-stars, and because of the *relatively* large spread in metallicity of the stars used for the calibration. The calibration by Nissen et al. (1987) could also be used, but this calibration is derived from M67, without any terms involving corrections for metallicity ( $\delta m_1$ ). On the other hand, the  $\delta m_1$  term in Olsen (1984) is most probably too large for stars more red than  $(b - y)_0 \approx 0^{\text{m}}500$  and we restrict our sample to stars with  $(b - y)_0 \leq 0^{\text{m}}500$ . As for the late F-stars in the Crawford (1975) calibration of the stars are restricted to those near the main sequence,  $\delta c_1 \leq 0^{\text{m}}2$ , spanning the  $\approx 2^{\text{m}}5$  width of the main sequence. The procedure described above is similar to what we have used before; thus the results in this paper may be directly compared with our previous results on distance and reddening (e.g. Jønch-Sørensen 1994, Jønch-Sørensen & Knude 1994, and Jørgensen & Jønch-Sørensen 1998) and also with other results based on Strömgren-photometry.

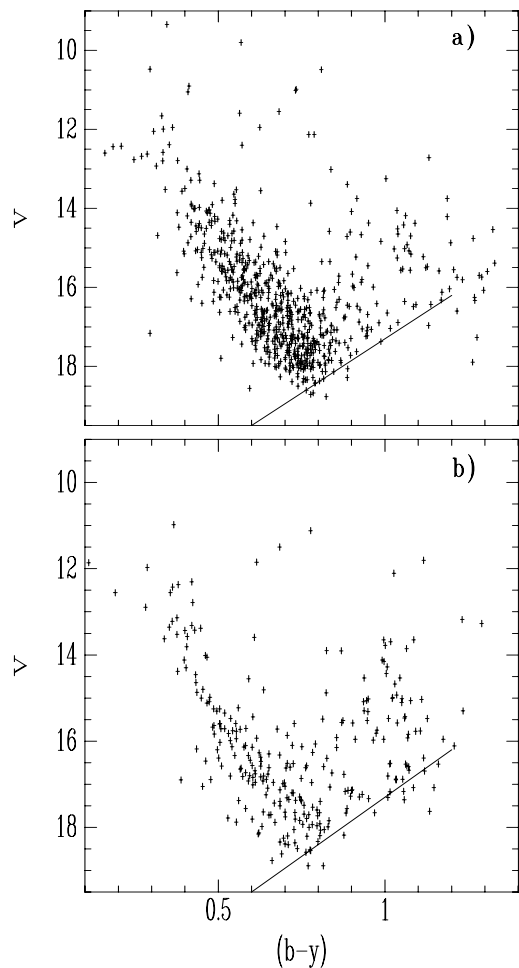


**Fig. 2a and b.** The Figure shows the  $(b - y) - V$ -diagrams for CG 30/31/38 field **a** and the reference field **b**, respectively. Only stars with full  $uvby - \beta$  photometric information have been included. The solid lines are eyeball fit to the lower envelope of the distribution used for an estimation of the maximum observable reddening in the two fields. The slopes of the two lines are identical because of identical exposure times of the frames in the two fields under consideration.

#### 4. The samples

A total of 698 and 526 stars were found with the full  $uvby - \beta$  data in the CG 30/31/38 and the reference field, respectively. Remembering the difference in field size we here get the first indication of a higher absorption in the CG 30/31/38 field with respect to the reference field. In Fig. 2 we show the  $(b - y) - V$ -diagrams of the samples with the complete  $uvby - \beta$  data. As expected the limiting magnitude varies with  $(b - y)$  because of the lower UV-flux emanating from late type- or reddened stars. The lines in Fig. 2 are eyeball fit to the lower envelope of the distribution. These relations are used in Sect. 6 when estimating the maximum observable reddening at a given distance as a function of intrinsic colour. According to the method described above (Sect. 3) 318 and 195 stars were classified as either A-, F- or G-type stars in the two fields, respectively. However, when the samples are limited to the stars with photometry strictly

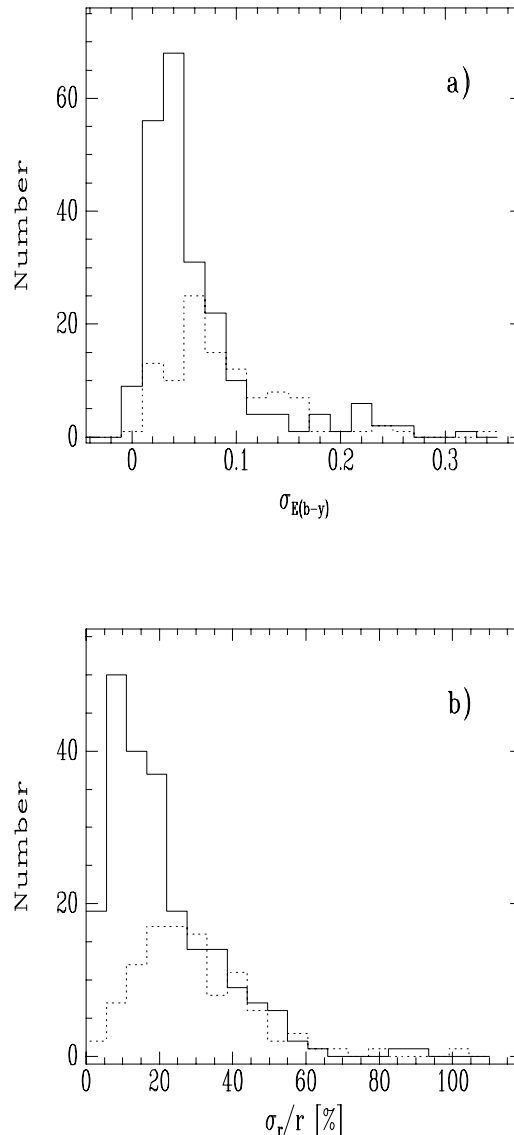


**Fig. 3a and b.** Histograms showing the distributions of  $\sigma_{E(b-y)}$  in magnitudes and the relative distance error ( $\sigma_r/r$ ) in % for the CG 30/31/38 field (solid line) and the reference field (dotted line).

inside the limits given by the calibrations mentioned above, we are left with 224 and 106 stars, respectively.

#### 5. The obtained accuracy

The accuracy of the derived reddenings and distances (or intrinsic colours and absolute magnitudes) are estimated by the propagation of the measuring errors into the calibration. The rather complex relation in the calibrations between the four indices  $(b - y)_0$ ,  $\beta$ ,  $m_0$  and  $c_0$  means that the uncertainty of the derived  $E(b - y)$  depends upon the position in the  $(\beta, m_1, c_1)$  space. Thus, the tight relation between apparent magnitude and uncertainties of the measurements of the individual magnitudes may not be found in the final uncertainties of the derived parameters. Furthermore, the two fundamentally different approaches in the calibrations by Crawford (1979) and Olsen (1988), and

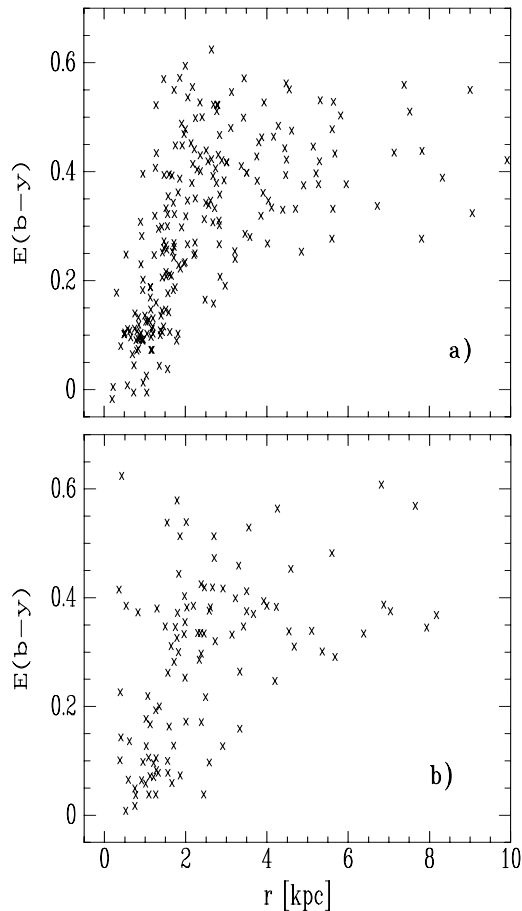


**Fig. 4a and b.** Distance and reddening for stars in **a** CG 30/31/38 (224 stars), and **b** the reference field (106 stars).

on the other hand Schuster and Nissen (1989), implies that the calculated formal errors may not be directly comparable.

In Fig. 3 we show the histograms of the distributions of  $\sigma_{E(b-y)}$  in magnitudes and the relative distance error ( $\sigma_r/r$ ) in % for both the CG 30/31/38 (solid line) and the reference field (dotted line) for stars with photometry strictly inside the limits given by the calibrations. The median of the  $\sigma_{E(b-y)}$  in the two fields are  $0^m04$  and  $0^m05$ , respectively. For the relative distance error the distributions peak at median values of 26% (CG-field) and 35% (reference field), respectively. The reason for the lower accuracy in the reference field is the smaller number of observations of each star (see Sect. 2). It should be noted, that these errors are purely formal errors calculated from the individual magnitude errors (which for most part are based on the standard error of the mean for multiple observations) propagated through the equations of the various calibrations. Errors from the transformation to the standard system has not been included, and it should be remembered that the calibrations have an intrinsic scatter. According to Nissen (1994) the intrinsic  $\sigma$  scatter of the calibrations are  $\approx 0^m010$  and  $\approx 15\%$  for  $E(b-y)$  and distance, respectively. On top of this, the effect of duplicity has not been included, but according to Nissen (1994) the error introduced is  $\leq 0^m025$  in  $(b-y)_0$  and up to 40% in the distance.

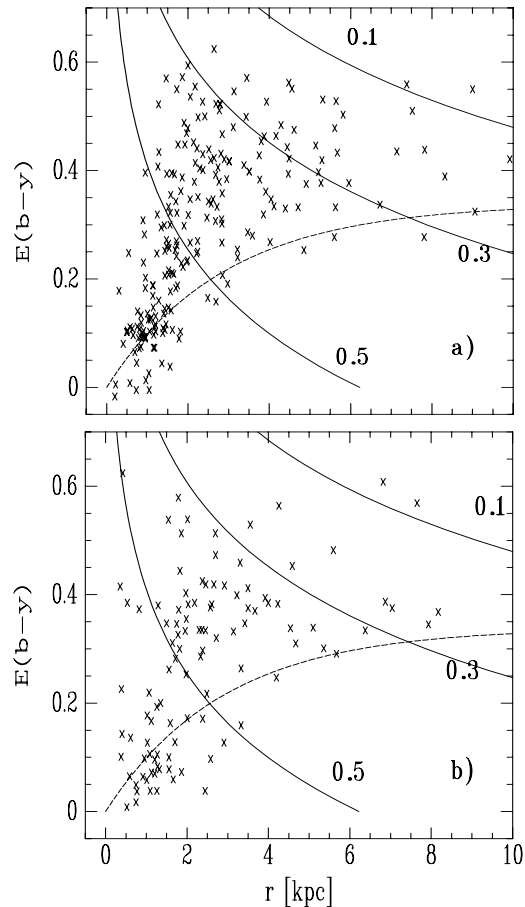


**Fig. 5a and b.** Same data as in Fig. 4a and Fig. 4b. Solid curves mark the maximum observable reddening as a function of distance for three values of  $(b-y)_0$ : 0.1 (A-stars), 0.3 (F-stars) and 0.5 (G-stars). The dashed curve is the distance-reddening relation described in the text.

## 6. Distance and reddening

One of the main objectives of this programme was to investigate if special features in the  $r - E(b-y)$ -diagram of the CG 30/31/38 field were present and could be used to derive distance to the complex of cometary globules. Thus, we start by comparing the diagram of CG 30/31/38 with both the corresponding result from the reference field and also with other similar investigations. First, we show the  $r - E(b-y)$ -diagrams for the two fields in Fig. 4. The large scale distribution along the sight line is as expected, e.g. Jønch-Sørensen (1994) and Jønch-Sørensen & Knude (1994), showing a general increase of  $E(b-y)$  with distance, with a lower envelope defining the minimum reddening caused by the diffuse interstellar medium confined to an exponential disk with a scale height of  $h_z \approx 140$  pc (Jønch-Sørensen 1994). The upper limit to the  $E(b-y)$  distribution does not necessarily reflect the complete dust absorption but is an effect of the limiting magnitude of the sample. This is illustrated in Fig. 5 where we show the same  $r - E(b-y)$ -diagrams with curves showing the maximum observable  $E(b-y)$  at a given distance for three different  $(b-y)_0$  values, corresponding approximately to the mini-

imum, the median and the maximum  $(b - y)_0$  values of the stars shown in the diagram. These colour limits are imposed by limitations in the calibrations. The curves are calculated using the  $(b - y) - V_{\text{lim}}$  relation mentioned in Sect. 4, and an absolute magnitude derived from the *standard dwarf sequence*, i.e. the  $(b - y)_0 - M_V$  standard relation for B- to K dwarfs (Crawford 1975, 1978, 1979; Hilditch et al. 1983; Olsen 1984). Thus, the maximum distance where a star of a given spectral type ( $(b - y)_0$ ) and a given reddening ( $E(b - y)$ ) may be observed, is calculated as:  $5 \log(r_{\text{max}}) = V_{\text{lim}} - M_V((b - y)_0) + 5 - 4.2E(b - y)$ , where  $V_{\text{lim}}$  is not a constant but given by the line in Fig. 2,  $V_{\text{lim}} = a_1((b - y)_0 + E(b - y)) + a_2$  where  $a_1$ ,  $a_2$  are the slope and intercept of the lines in Fig. 2. Thus, the curves in Fig. 5 confine the area in the  $r - E(b - y)$ -diagram where an unevolved main sequence star of solar metallicity may be observed.

The minimum reddening at large distance is well represented by the dashed curve in Fig. 5. This curve represents the expected distance-reddening relation calculated using the model described in Jönch-Sørensen (1994). The parameters for the diffuse medium entering the model in Fig. 5 are: a scale height of 140 pc, a scale length of 4000 pc and a local normalization of the density  $n_0$  of 0.25 H-atoms/cm<sup>3</sup>. This is in agreement with the result found in a nearby field  $(l, b) = (262, +4)$  (Jönch-Sørensen & Knude 1994) where the minimum reddening was described by the same model with  $n_0 = 0.33$  H-atoms/cm<sup>3</sup>. The total minimum reddening through half the disk at this position is  $E(b - y) \approx 0^{\text{m}}30$  along the line of sight. Using the relation,  $A_V = 4.2E(b - y)$ , this corresponds to  $A_V = 1^{\text{m}}26$ . According to Yamaguchi et al. (1999) the area on the sky containing the reference field, is not completely free from molecular emission as expected from visual inspection. In fact they find that the intensity of the millimetre <sup>12</sup>CO ( $J = 1 - 0$ ) line is  $\sim 7$  K km/s somewhere inside the reference field. Using a ratio between the column density,  $N(H_2)$ , and the intensity,  $I(^{12}\text{CO})$ , of  $2.3 \cdot 10^{20}$ , we find a value of  $N(H_2) \sim 1.6 \cdot 10^{21}$  cm<sup>-2</sup>. The visual extinction can be derived using the standard relation between  $A_V$  and the H<sub>2</sub> column density of  $A_V = N(H_2)/10^{21}$ . Consequently, the visual extinction, coming from the molecular material, is  $\sim 1^{\text{m}}6$  along the line of sight towards the reference field. However, this high extinction is possibly not representative for the whole reference field.

The large scale behaviour of the distance-reddening distribution for the CG 30/31/38 and the reference fields are very similar to each other as seen in Fig. 4a and Fig. 4b. Furthermore, it is also similar to what is found in other fields at very different positions in the Galactic disk (see below). However, there is a difference when dividing the CG 30/31/38 sample into areas inside the region of the cometary tails and outside the tail region. We selected stars from three regions (see Fig. 6) of approximately the same size. In Fig. 7a–c we clearly show that the area in the *tail free* part of the CG 30/31/38 field experience a lower reddening at large distances. Because of the limiting magnitude (see Fig. 5) it is not possible to estimate the true maximum or mean reddening for distances above approximately 3 kpc, but it is obvious that the reddening is at least  $0^{\text{m}}15$  (corresponding to  $A_V \approx 0^{\text{m}}63$ )

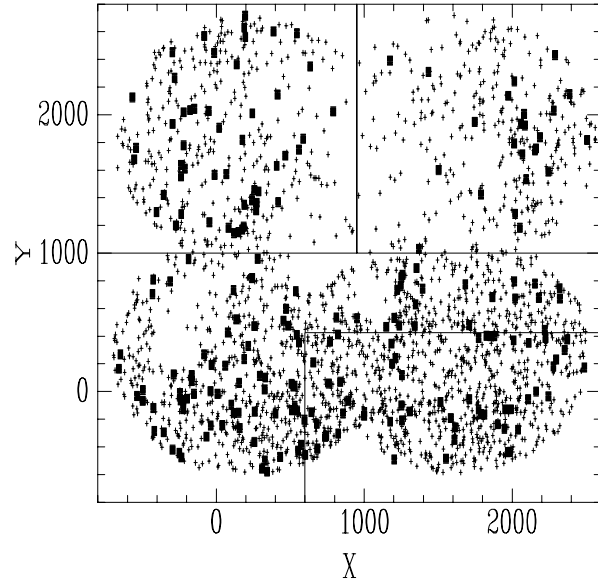


**Fig. 6.** The observed stars in the CG 30/31/38 field.  $X$  and  $Y$  are the pixel coordinates in the combined system. North is up, east to the left; one pixel corresponds to  $0^{\text{m}}39$ . The three boxes mentioned in Sect. 6 are shown. The small symbols represent stars for which we have obtained at least  $b$  and  $y$  magnitudes. Stars with derived distance and reddening are marked by filled boxes.

higher in the tail than outside, which we interpret to be caused directly by the molecular material in the tails. The tail region of the complex of cometary globules must on average contribute with much more than this, because the least reddened stars are observed in less obscured directions of the highly fragmented material in the tails. Note that Knude et al. (1999) proposed that an absorption feature with  $A_V \approx 3^{\text{m}}6$  at a distance of 200 pc may be associated with the wind blown tail of CG 31. Such a high absorption (corresponding to  $E(b - y) \approx 0^{\text{m}}9$ ) will bring stars outside the observable area (Fig. 5) and since we do see stars in the tail region beyond 1 kpc, we may conclude that this large absorption is not representative for the whole tail region, in fact we do find 4 stars with distances larger than 1 kpc in the box confined by the pixel interval  $[500:2000, 1500:2000]$  (see Fig. 6) used by Knude et al. (1999) to identify a feature at 660 pc having  $A_V = 2^{\text{m}}8$ .

Apart from the higher reddening at large distances another clear difference is that the tail region shows a transition from low- to high reddening occurring at  $\approx 1$ -1.5 kpc. Note that this transition is also seen in the *tail free* region and in the reference field, but the transition zone is much broader here and less dramatic. The difference may be an imprint of an absorption feature associated with the tails of the CG's, and will be discussed further in Sect. 6.1.

### 6.1. The nearest 2 kpc

The CG 30/31/38 complex is expected to be situated at a distance of 200–450 pc (thereby including the lower and upper distances used in the literature), and in combination with the

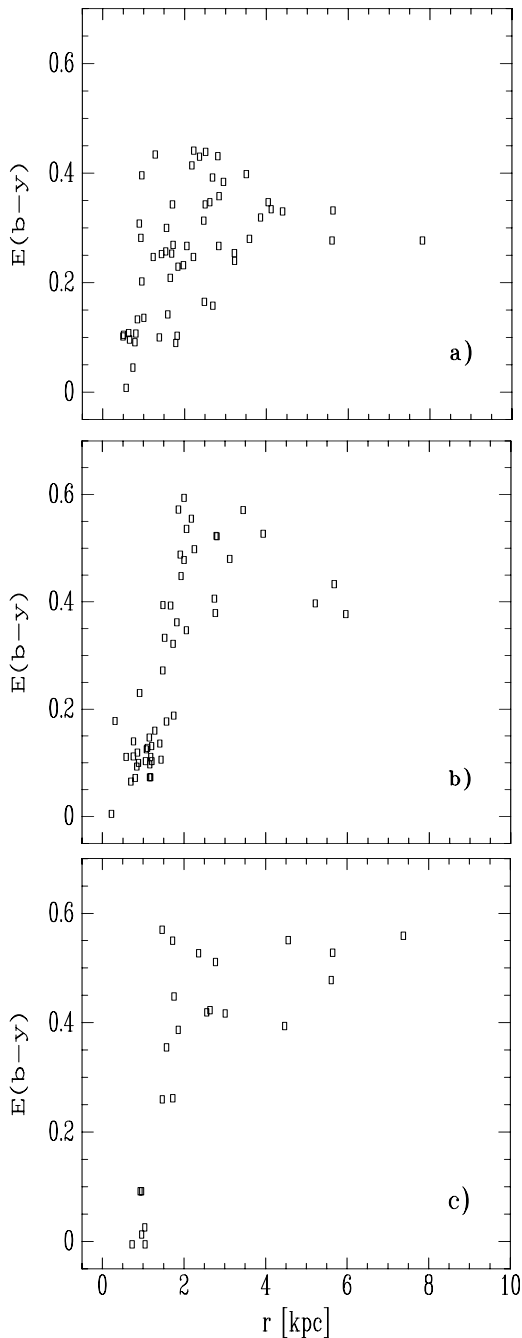


**Fig. 7a–c.** Distance and reddening in the three boxes of Fig. 6. **a** corresponds to the lower right part of the field. **b** is the eastern part of the tail, and **c** is the western part of the tail region.

above mentioned *transition area* at  $\approx 1\text{--}1.5$  kpc we will therefore now concentrate on the nearest 2 kpc. Fig. 8 is the same data as in Fig. 5 but here distances pertaining to the volume within 2 kpc. There is nothing in the distribution of reddening and distances that indicates a difference between the field with the CG-complex and the reference field without *enhanced molecular emission*. However, the “jump” at 300–400 pc is most prominent for the reference field. Although it is only based on an excess of three to four stars from the reference field, it should

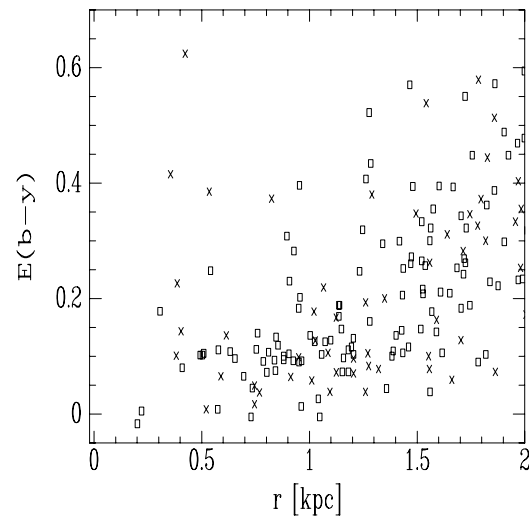


**Fig. 8.** As Fig. 4, a close up of the first 2 kpc. Boxes are the CG 30/31/38 stars and crosses the stars from the reference field.

be remembered that we only sample  $\approx 1/3$  of the volume in the reference field with respect to the CG 30/31/38 field.

In both fields we find unreddened stars to a distance of 1.1 kpc where a *jump* in reddening occurs. The minimum reddening increases to  $E(b-y) \approx 0^{\text{m}}05$  and the upper envelope of the  $r - E(b-y)$  relation increases from  $E(b-y) \approx 0^{\text{m}}4$  to  $\approx 0^{\text{m}}6$ . Before investigating this further, we should again check if the feature seen in Fig. 8 is a *normal* distribution, in the sense that it is what to be expected from a field where the reddening is dominated by the omnipresent diffuse interstellar medium. To do this we first compare with other similar CCD  $uvby - \beta$  programmes. In Fig. 9 we show the same data as in Fig. 8 together with distance and reddening results for stars found in 10 other fields with galactic coordinates: (196,+28), (340,+21), (350,+12), (356,-40), (44,-52), (270,+35) (Jønch-Sørensen 1995); (262,+4) (Jønch-Sørensen & Knude 1994); (281,+11) (Jørgensen & Jønch-Sørensen 1998), (151,-13) (Jørgensen & Jønch-Sørensen 2000), and finally (180,-1) in Jønch-Sørensen (2000). In Fig. 9a we show the distance versus measured  $E(b-y)$  and in Fig. 9b the reddening has been corrected in order to compensate for the different galactic latitudes of the 10 comparison fields (longitude and distance have remained fixed). The correction is calculated for each field using the model described in Jønch-Sørensen (1994), thus correcting the reddening from the measured one to what it would have been at the same latitude as CG 30/31/38 if it is only caused by the diffuse interstellar medium.

Looking at either Fig. 9a or Fig. 9b it seems that we do not detect any sharp features in the  $r - E(b-y)$ -diagram for the CG 30/31/38 field. However, in Fig. 9b one can again notify an excess of stars from the 10 “other” fields at  $E(b-y) \gtrsim 0^{\text{m}}15$  and  $r \leq 0.9$  kpc compared to the reference field but especially the CG 30/31/38 field. The total area on the sky covered by the 10 fields is approximately 2.5 times the size of the CG 30/31/38 field, and they are all situated at larger angular distances from the Galactic plane, meaning that the star density is lower. Thus, if we

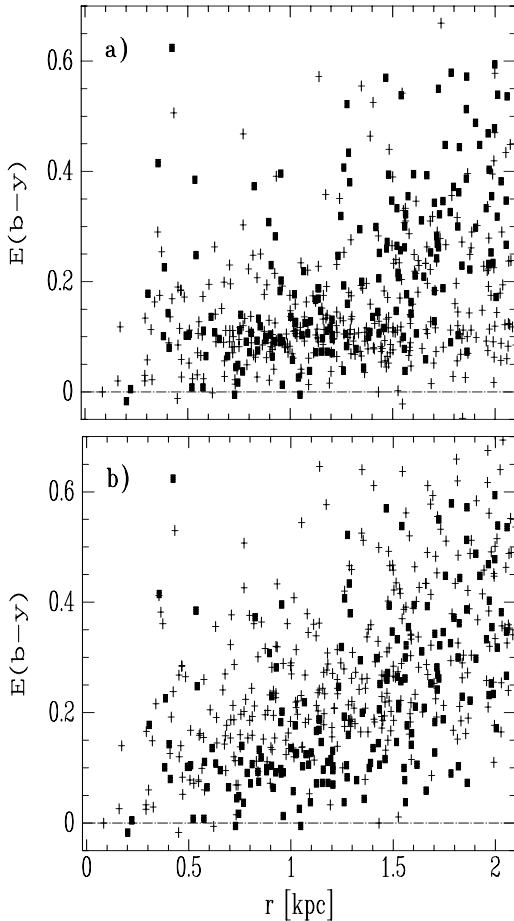


**Fig. 9a and b.** Same data as in Fig. 8 (our combined data are indicated by filled boxes), but with the inclusion of 10 other fields described in the text (+). **a** is a plot of the distance versus measured  $E(b - y)$  for the stars as taken from the literature, whereas in **b** we have corrected the reddening to be influenced only by the local interstellar medium as seen towards CG 30/31/38, thereby compensating for the different galactic latitudes in the samples.

correct for the lower star density at higher latitudes, we should expect an even larger number of stars in the area characterised by  $r \lesssim 1$  kpc and  $E(b - y) > 0^m15$ , than seen in Fig. 9b. The number of stars with  $r < 0.9$  kpc and  $E(b - y) < 0.15$  is 24 and 8 for CG 30/31/38 and the reference field respectively, in perfect agreement with the difference in field sizes. For  $r < 0.9$  kpc and  $E(b - y) > 0.15$  the number of stars are 3 and 5 respectively. And the three stars in the CG 30/31/38 field with  $r < 0.9$  kpc and  $E(b - y) > 0.15$  are situated in areas outside the visible tails. As noted in the discussion of Fig. 7 this may be caused by the appearance of (distinct) absorption features within the first kpc along the line of sight. Stars within 1 kpc from the Sun may experience a reddening that is too high for the star to be detected in our sample, but at larger distances (and thus larger volume in space) there is a sufficient number of stars for some of them to be spotted through holes in the patchy medium. We expect that it is the wind blown tails of the CG's that are responsible for the smaller number of nearby, reddened stars in the CG 30/31/38

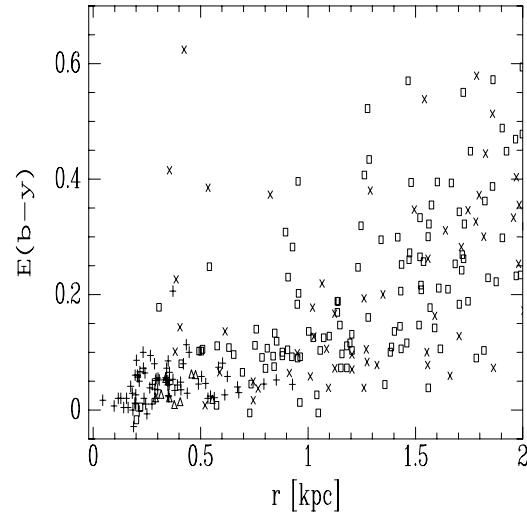


**Fig. 10.** As Fig. 8, now including data from  $16^\circ$  in SA 171 (Franco 1989) indicated by (+) and 9 B-stars near  $\gamma^2$ -Vel (Franco 1990) marked with triangles.

field with respect to the reference field. In addition to this, we do also expect another excess absorption affecting both fields, because the number of stars in the reference field with  $r < 0.9$  kpc and  $E(b - y) > 0.15$  is lowered by a factor of 3–4 with respect to what we expect from the 10 comparison fields. In Knude et al. (1999) three such features were proposed, the one mentioned earlier at 200 pc with  $A_V \approx 3^m6$ , one at 400 pc with  $A_V \approx 0^m5$  and finally one at 660 pc having  $A_V \approx 2^m8$ .

The rather small volume we sample in our  $\approx 1/6^\circ$  field to 500 pc is too small to contain enough A- to G-stars to make any decisive conclusions from the  $r - E(b - y)$ -diagram. Thus, we try to compare our results with those obtained by Franco (1989) extending over a much wider area. His sample consists of photoelectric  $uvby - \beta$  photometry of B-, A- and F-stars brighter than  $\approx 11^m$  in 10 Selected Areas on the sky. One of his observed areas,  $16^\circ$  in SA 171, covering the globules CG 8/9/10, is centered at  $(l, b) = (258, -11)$ , thus  $10^\circ$  from our CG 30/31/38 field. In Fig. 10 we show his data (+) from SA 171 together with our results. The data for his bright stars collected from a large area on the sky forms a nice continuation of our deep photometry of stars in the same general direction of the Galaxy. The magnitude limit of the data by Franco is  $\approx 11^m$  and therefore he cannot observe stars with  $E(b - y) \approx 0^m2$  to distances beyond  $\approx 400$  pc. Note that Franco (1990) supposed that the increase in colour excess at approximately 200 pc is caused by dust within the near edge of the Gum Nebula, which in combination with the angular size of the nebula, led him to derive a distance of 290 pc to the center of the Gum Nebula. Also shown in Fig. 10 are the results from Franco (1990) of distance and reddening of 9 B-stars located somewhere in the  $\gamma^2$ -Velorum region.

## 6.2. Late type dwarfs

Since we do not have enough A- to early G-type stars with accurate measurements of distances and reddening, at distances

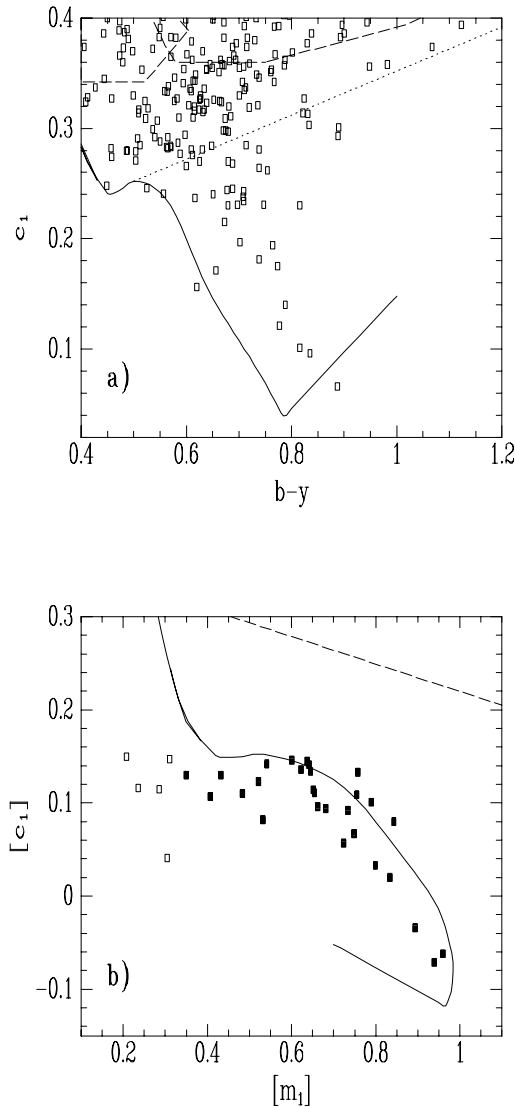


**Fig. 11a and b.** In **a** we show the  $(b - y) - c_1$  diagram for the stars in CG 30/31/38. The solid curve is the unreddened standard dwarf sequence (references in text), The dashed curve is the mean relation for G0–M4 (LC III) stars (Olsen 1984). The dotted curve is parallel to the reddening vector and limit the area from where we select our candidate late type dwarfs (see text). In **b** the  $[m_1] - [c_1]$  diagram of the stars selected from **a**, with  $(b - y) \geq 0^m5$  and  $c_1$  below the dashed line, is shown. The filled symbols are the stars that lie close to the standard dwarf sequence (solid curve) and are selected as certain late type (K) dwarfs. The dashed curve is the mean relation for M (LC III) stars (Olsen 1984).

below 500 pc, we may look for more frequent later type stars in this range. As noted in Sect. 3 we have restricted our primary sample of A-, F- and early G-type stars to those having  $(b - y)_0 \leq 0^m500$ . We may still get reliable information from later type stars (late type dwarfs) although the situation as regards reliable calibrations of  $(b - y)_0$  and  $M_V$  is less favourable, basically because the  $\beta$ -index loses sensitivity. However, we may get an estimate of the reddening and distances using other criteria, following Olsen (1984).

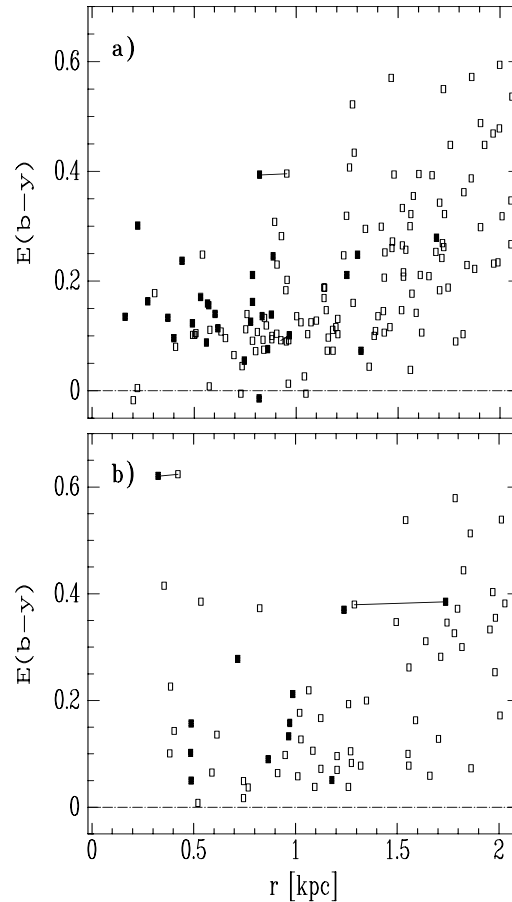


**Fig. 12a and b.** Distance and reddening for stars closer than 2 kpc. Open symbols are the A-G type stars presented in the previous figures, filled symbols are the late type dwarfs selected as described in the text. **a** the CG30/31/38 field, and **b** the reference field. The two connected symbols in **a** and **b** correspond to the same star with distance and reddening derived from both methods.

We first choose stars in the  $(b - y) - c_1$  diagram on the basis that for  $(b - y)_0 \geq 0^m5$  the standard lines of unreddened stars of LC V and III begin to separate (Fig. 11a). We draw a line from the standard dwarf sequence at  $(b - y)_0 = 0^m50$ ;  $c_0 = 0^m252$  following the reddening vector with a slope of 0.2 ( $E(c_1) = 0.2E(b - y)$ ). We require that G-K-dwarf candidates for a given  $(b - y)$  should have  $c_1$  less than the value given by the line. These stars are very likely G- or K-dwarfs and we do not expect any significant contribution from LC IV or more evolved stars. This is confirmed in the  $[m_1] - [c_1]$  diagram (Fig. 11b). After this first selection we find 46 and 18 candidates in the CG 30/31/38 and reference field, respectively. Next we require that the stars should have indices within  $\pm 0^m1$  of the  $[m_1] - [c_1]$  standard relation (inspired by Olsen 1984, Fig. 7). In this way we eliminate most “peculiar” stars, such as Barium and CH stars, ending up with 30 and 14 stars, respectively. For this subsample we estimate  $(b - y)_0$  and  $M_V$  (ZAMS) from interpolation of  $[m_1], [c_1]$  according to Olsen (1984; Table VI).  $M_V$  (ZAMS) were corrected for metallicity ( $\delta m_1$ ) and

**Table 2.** Photometry of selected G dwarfs. The “Method 1 calibration” is discussed in this section, whereas the “Method 2 calibration” is described in Sect. 3.

Method 1 calibration		Method 2 calibration	
$E(b - y)$	$r$ [pc]	$E(b - y)$	$r$ [pc]
0.101	967	0.092	925
0.394	821	0.396	954
0.621	325	0.624	423
0.385	1738	0.380	1290

evolution ( $\delta c_1$ ) according to Olsen (1984; Eq. (5)), involving however only small corrections for most stars.

The method can be evaluated because the samples of G-K dwarfs contain two stars in both fields that were also classified as G-stars and had  $E(b - y)$  and  $r$  derived by the calibrations described in Sect. 3. The results are listed in Table 2 and the stars are marked in Fig. 12 with connected symbols. The two methods are very consistent with respect to estimation of intrinsic colour; the somewhat larger discrepancy with regards to distance is most probably an effect of the more uncertain correction for evolution and metallicity in the calibration by Olsen (1984) for the late type dwarfs.

Fig. 12 shows the results for the A-, F- and G-stars (as in Fig. 8) together with the results for the late type dwarfs, for both CG 30/31/38 and the reference field. Apparently the late type stars show the same  $r - E(b - y)$  relation as the earlier types, a *jump* at 200 pc may be inferred, but still the number of stars closer than 400 pc is rather small. The total lack of stars closer than approximately 300 pc in the reference field is very likely caused by the smaller beam size and we believe that the apparently higher reddening in the reference field than in the CG 30/31/38 field is in fact caused by high absorption features in the direction of CG 30/31/38 amounting to at least  $E(b - y) = 0^m4$  ( $A_V = 1.7$ ) and thus making these kind of stars,  $0^m3 \leq (b - y)_0 \leq 0^m5$ , undetectable in our sample (consult Fig. 5).

### 6.3. $V$ and $I$ photometry for selected dwarfs

In two 17 minutes  $V$  and  $I$  exposures two faint stars located towards the most dense part of CG 31A were identified (Fig. 13). Since  $A_V$  for CG 31A is expected to exceed 10 magnitudes, a determination of their distances would give us a lower distance limit to the globules. These stars were more than 1 magnitude fainter than the limit for automatic detection (in DAOFIND) in our first observations, and aperture magnitudes were derived on manual basis in IRAF and transformed to the standard system using 8 brighter nearby stars. Despite the less accurate photometry, the faint stars proved interesting because of their location and their derived colours. Therefore, additional deeper observations were performed in Nov. 1999, where we obtained the following: 2  $V/45$ min, 2  $V/30$ min, 2  $I/30$ min, and 1  $I/20$ min exposures centred on CG 31A. Based on the transformations discussed in Sect. 2.2, we derived the following magnitudes and colours for

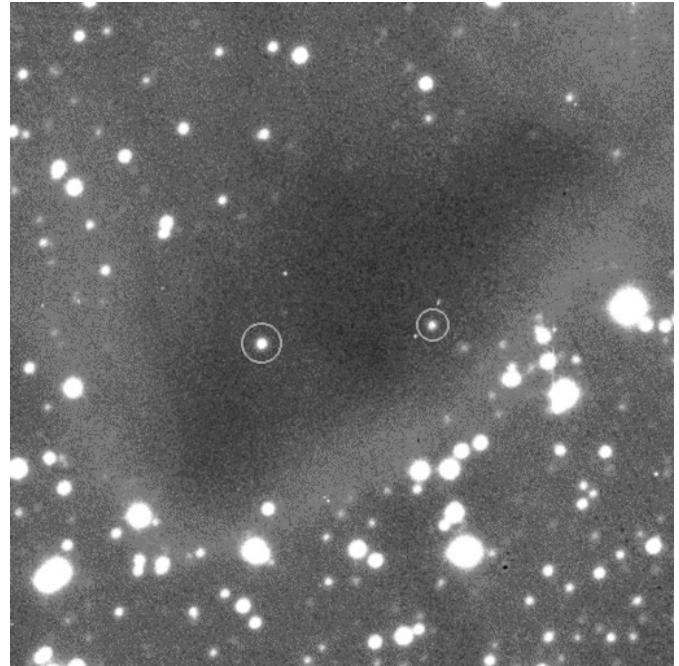


**Fig. 13.** An  $I$ -band image showing the head of CG 31A, as well as the location of the two reddest dwarfs marked by white circles. The area shown corresponds to  $3'3 \times 3'3$ .

these two stars:  $V = 22^m174$  [0.060],  $(V - I) = 3^m839$  [0.061] and  $V = 23^m575$  [0.052],  $(V - I) = 4^m157$  [0.052], respectively. If unreddened these colours correspond to spectral types M5 and M6 (Bessel 1990). The two stars are situated towards the densest part of CG 31A, Fig. 13, where we find no other stars brighter than  $V \approx 23$  and  $I \approx 23$  and we conclude that a conservative estimate of the visual absorption in these very dense areas is  $A_V \gtrsim 15^m$ . We feel confident that these stars are foreground stars, and thus situated at distances well below 400–500 pc. For stars closer than 400 pc we expect a reddening of  $E(b - y) = 0 - 0^m1$  (see Fig. 10) corresponding to  $A_V = 0 - 0^m42$  and  $E(V - I) = 0 - 0^m15$  (using the relation  $A_V = 2.8E(V - I)$ ). Reid (1991) derived a relation given by

$$M_V = (2.89 \pm 0.20) + (3.37 \pm 0.07)(V - I)_0$$

a calibration which is valid for  $(V - I) \in [1, 4.5]$ , and applying this to our two stars we find distances of 186 pc and 216 pc, respectively for  $A_V=0$  and 193 pc and 216 pc for  $A_V=0.42$ . Note that the reason why increasing  $A_V$  yields larger distances to the stars is that the slope of the  $M_V - (V - I)_0$  relation is steeper than the  $A_V - E(V - I)$  relation.

Assuming the stars are *background* stars, they have to penetrate  $A_V \gtrsim 15^m$ , corresponding to  $E(V - I) \gtrsim 5.4$ , which at a distance of 500 pc (assumed to be behind CG 31A) would require an absolute magnitude of  $M_V \lesssim -1^m5$ . Thus we cannot completely exclude that these two stars are very blue and distant super giants. Nor can we exclude that what we see is two stars of a more frequent type through two holes in the head of CG 31A. However, both alternatives seem very implausible to us, and we conclude that those two stars are nearby, red dwarf stars, situ-

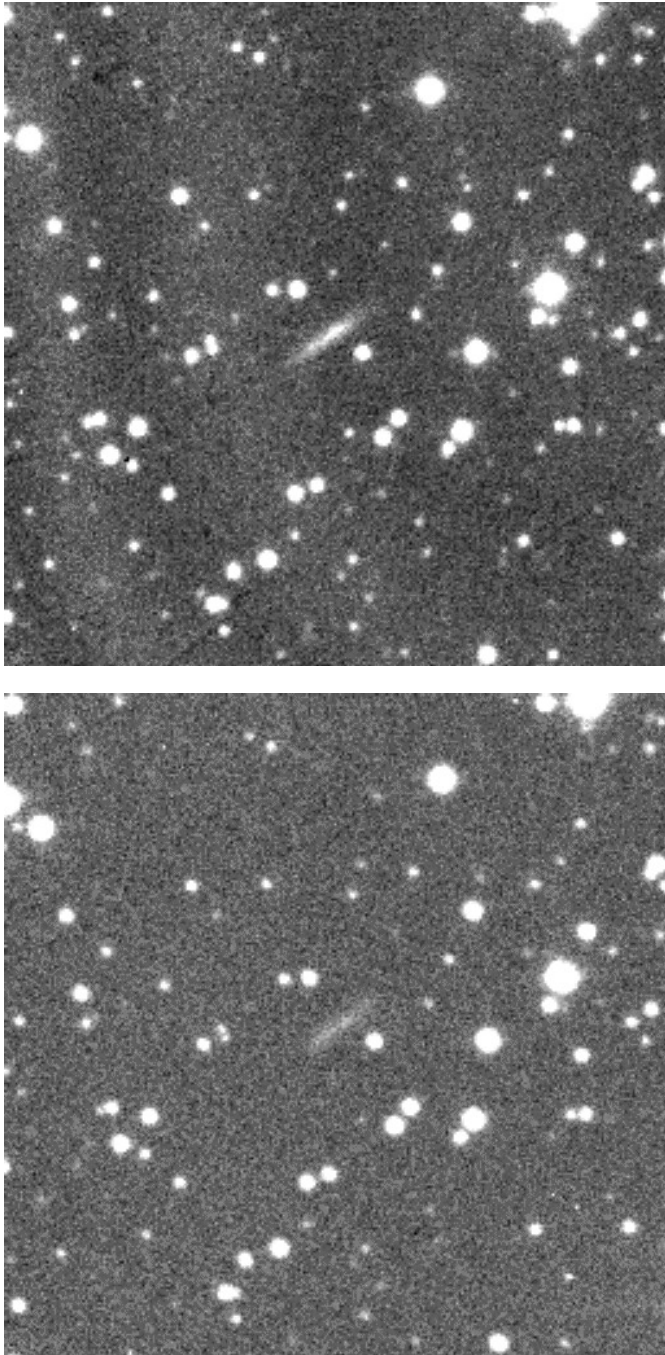


**Fig. 14.** A small section ( $1'.7 \times 1'.7$ ) of the reference field in the *I*-band (top) and in the *V*-band (bottom), both integrated in 10 minutes, showing a newly discovered galaxy located at  $b \sim -1.6^\circ$ .

ated between the Sun and CG 31A, giving us an opportunity to estimate a *minimum* distance to the head of the cometary globule. We conclude, that the minimum distance to CG 31A is of the order  $215 \pm 40$  pc, the errors based on the quoted photometric accuracy. This is in agreement with the distance derived by Knude et al. (1999) of  $200 \pm 40$  pc.

During close inspection of the reference field in the *I*-band and *V*-band, both having an exposure time of 10 min,

we found an edge-on galaxy (Fig. 14), presumably not previously detected. This was an unexpected surprise to us, since the high reddening at such low galactic latitude normally prevents lights from external galaxies to penetrate, but it demonstrates again that the interstellar medium is rather patchy. By fitting an aperture to the central parts, we found the following magnitudes and colours for the galaxy:  $V_{\text{std}} = 22.529[0.033]$ , and  $(V - I)_{\text{std}} = 2.600 [0.035]$ . If we subtract the minimum reddening found in the reference field (Fig. 4b), we find a value of  $(V - I)_0 = 2.15$  for the faint galaxy.

These latter results are preliminary, but we intend to make further observations in the future, using a larger telescope than the danish 1.54 m, in order to clarify the nature of this galaxy.

We also examined the CG-field in order to find additional galaxies, but without success.

## 7. Discussions

We have presented and discussed the second part of our photometric study of the CG 30/31/38 complex. In the first part described in Knude et al. (1999) we used the  $(V, V - I)$  diagrams to find indications of absorption features at distances of 200, and 660 pc, respectively, the former was suggested to be related to the wind blown tail of the cometary globules. In this paper we have presented deep CCD *uvby* -  $\beta$  photometry towards the CG 30/31/38 region as well as a reference field. We have obtained distance and reddening for as many stars as the calibration allowed in those two fields. However, because of the small volume sampled, we do not find quite enough stars closer than  $\approx 600$  pc, with a favourable location, to detect these features in the  $r - E(b - y)$  diagrams. However, from the  $(V, V - I)$  data for two newly discovered M-dwarfs in front of CG 31A, we may derive a minimum distance to the globule of  $215 \pm 40$  pc, possibly a representative distance estimate for the whole complex of globules. This is further supported by the fact that the systemic (LSR) velocity of the CG 30/31/38 globules is  $6 \text{ km s}^{-1}$  (Nielsen et al. 1998), which makes it likely that they belong to the same complex, are located at a common distance, and are exposed to the same ionizing source(s).

The  $r - E(b - y)$  diagram for both the field containing CG 30/31/38 and the nearby reference field are very similar, and compared to fields situated in different directions of the Galaxy, we see an indication of a deficit of stars closer than  $\approx 1$  kpc with  $E(b - y) \geq 0^{\text{m}}2$ , most prominent in the CG 30/31/38 region. This may be interpreted as the cumulative effect of the strong absorption features found by Knude et al. (1999), because the high absorption in these features, adding up to more than  $E(b - y) = 0^{\text{m}}9$ , brings the stars out of the observable area defined by our limiting magnitude ( $V \sim 19$ ). The similarity between the  $r - E(b - y)$  diagrams for the CG 30/31/38 and the reference field indicates that the  $r \leq 1$  kpc “features” are common to the general area and not related to the cometary globules.

From distant stars we find that the wind blown tails add a reddening of at least  $E(b - y) \approx 0^{\text{m}}15$  (corresponding to  $A_V \approx 0^{\text{m}}65$ ) relative to the *tail-free* region. The minimum reddening

through half the Galactic disk is  $E(b - y) = 0.3$  corresponding to  $A_V \approx 1.26$  in the tail free region, along the line of sight.

The spatial geometry and the interplay of the ISM and ionizing sources in the Gum-Vela region is extremely complicated, as notified from previous published articles, most of them contradicting each other one way or the other. That is why an *indirect* distance estimate to the globules is of very limited use. We have tried in this work and in Knude et al. (1999), to make a *direct* estimate of the distance to the globules, based on  $uvby - \beta$ - and  $(V, V - I)$  photometry. One of the obvious advantages in doing this, is to establish which source(s) is responsible for the cometary appearance of the CG's. If the distance is 400–450 pc, most likely Vela OB2 and  $\zeta$ -Pup are the primary sources of ionizing radiation. However, as stated before, the most likely distance is 200–250 pc, making the  $\gamma^2$ -Vel system ( $r \sim 258$  pc) responsible for the photo evaporating tails. We favour the latter suggestion and feel rather confident that the distance is closer to 200–250 pc than to 450 pc - the argument is as follows: from spectroscopic radio observations of the CO molecule (Nielsen et al. 1998), we have shown that essentially no velocity gradient from the head to the tail of the globules is present, indicating that the tails are more or less situated perpendicular to the line of sight. If the CG's were located behind the ionizing source, we would expect the globules to be illuminated on the front side, which does not seem to be the case from inspection of the obtained images, including  $V$  and  $I$  frames (see Fig. 1 for a Balmer line exposure). It seems more plausible that they are illuminated by  $\gamma^2$ -Vel from the direction opposite the tails, which causes the existence of bright rims. These arguments and previous work by Knude et al. (1999) makes it plausible that the globules are located marginally closer to us than the  $\gamma^2$ -Vel system giving rise to the cometary shape and eventually complete evaporation of the CG's.

Following this scenario we can tentatively conclude that the distance to the globules is most likely in the vicinity of 200–250 pc, in agreement with Knude et al. (1999).

*Acknowledgements.* We would like to thank IJAF for granting us the observing time in 1997 and providing travel funds for the investigation of the CG 30/31/38 region. Alan S. Nielsen thanks The Niels Bohr Institute for Astronomy, Geophysics and Physics for a PhD scholarship. H. Jønch-Sørensen thanks the Carlsberg Foundation for financial support. Søren Larsen is thanked for performing the additional  $V$  and  $I$  observations in Nov. 1999. We gratefully acknowledge Dr. H.C. Bhatt for carefully reading the manuscript.

## References

- Bertoldi F., 1989, ApJ 346, 735  
 Bertoldi F., McKee, C.F., 1990, ApJ 354, 529  
 Bessel M.S., 1990, A&AS 83, 357  
 Bhatt H.C., 1993, MNRAS 262, 812  
 Brandt J.C., Stecher T.P., Crawford D.L., Maran S.P., 1971, ApJ 163, L99  
 Crawford D.L., 1975, AJ 80, 955  
 Crawford D.L., 1978, AJ 83, 48  
 Crawford D.L., 1979, AJ 84, 1858  
 Crawford D.L., Barnes J.V., 1970, AJ 75, 978  
 de Zeeuw P.T., Hoogerwerf R., de Bruijne J.H.J., Brown A.G.A., Blaauw A., 1999, AJ 117, 354  
 Franco G.A.P., 1989, A&AS 78, 105  
 Franco G.A.P., 1990, A&A 227, 499  
 Gott J.R., Ostriker J.P., 1971, in: Maran S.P., Brandt J.C., Stecher T.P., The Gum Nebula and Related problems, NASA SP-322, p. 42  
 Graham J.A., 1982, PASP 94, 244  
 Grønbech P.J., Olsen E.H., Strömgren B., 1976, A&AS 26, 155  
 Hawarden T.G., Brand P.W.J.L., 1976, MNRAS 426, 669  
 Henning T., Launhardt R., 1998, A&A 338, 223  
 Hilditch R.W., Hill G., Barnes J.V., 1983, MNRAS 204, 241  
 Jønch-Sørensen H., 1993, A&AS 102, 637  
 Jønch-Sørensen H., 1994, A&AS 108, 403  
 Jønch-Sørensen H., 1994, A&A 292, 92  
 Jønch-Sørensen H., 1995, A&A 298, 799  
 Jønch-Sørensen H., Knude J., 1994, A&A 288, 139  
 Jørgensen I., Jønch-Sørensen H., 1998, MNRAS 297, 968  
 Jønch-Sørensen H., 2000, in preparation  
 Jørgensen I., Jønch-Sørensen H., 2000, in preparation  
 Knude J., Jønch-Sørensen H., Nielsen A.S., 1999, A&A 350, 985  
 Landolt A.U., 1983, ApJ 88, 439  
 Lefloch B., Lazareff B., 1994, A&A 289, 559  
 Lefloch B., Lazareff B., 1995, A&A 301, 522  
 Lefloch B., Lazareff B., Castets A., 1997, A&A 324, 249  
 Manfroid J., Sterken C., 1992, A&A 258, 600  
 Nielsen A.S., Olberg M., Knude J., Booth R.S., 1998, A&A 336, 329  
 Nissen P.E., Twarog B.A., Crawford D.L., 1987, AJ 93, 634  
 Nissen P.E., 1994, Rev. Mex. Astron. Astrofis. 29, 129  
 Olsen E.H., 1983, A&AS 54, 55  
 Olsen E.H., 1984, A&AS 57, 443  
 Olsen E.H., 1988, A&A 189, 173  
 Oort J.H., Spitzer L., 1955, ApJ 121, 6  
 Perry C.L., Olsen E.H., Crawford D.L., 1987, PASP 99, 1184  
 Pettersson B., 1984, A&A 139, 135  
 Reid N., 1991, AJ 102, 1428  
 Sahu M.S., 1992, Ph.D. thesis  
 Schaerer D., Schmutz W., Grenon M., 1997, ApJ 484, L153  
 Schuster W.J., Nissen P.E., 1988, A&AS 73, 225  
 Schuster W.J., Nissen P.E., 1989, A&A 221, 65  
 Strömgren B., 1963, in: Strand (ed.), Stars and Stellar Systems  
 Thoraval S., Boissé P., Duvert G., 1997, A&A 319, 948  
 van der Hucht K.A., Schrijver H., Stenholm B., et al., 1997, New Astronomy 2, 245  
 Yamaguchi N., Mizuno N., Moriguchi Y., et al., 1999, PASJ 51, 765